

PACS numbers: 42.55.Lt; 42.60.Lh
DOI: 10.1070/QE2008v038n01ABEH013522

On the nature of phantom currents in the active medium of self-contained metal atom transition lasers

N.A. Yudin, V.B. Sukhanov, F.A. Gubarev, G.S. Evtushenko

***Abstract*. The amplitude and duration of currents flowing in a discharge circuit of a laser are studied depending on the parameters of the active medium and excitation conditions. It is shown that a phantom current is determined by the specificity of charging the capacitive component of the impedance of a gas-discharge tube (GDT) in the laser. In this case, the current flowing through a thyratron is the charging current of the capacitive components of the impedance of the discharge circuit of the laser. As a result, currents flowing through the thyratron and GDT are substantially different. The active medium is at the same potential during the existence of the phantom current, which prevents prepulse electrons in the plasma from accumulating the energy required to realise inelastic collisions in the active medium.**

Keywords: *copper vapour laser, phantom current.*

1. Introduction

The active medium of repetitively pulsed self-contained metal atom transition lasers is characterised by a high prepulse electron concentration n_e. It is assumed that phantom currents flowing through the active medium are the indicator of n_e in these lasers [1, 2]. The phantom current is observed at the initial stage of the discharge development and is interpreted [1] as a current produced by prepulse electrons, which have not acquired the energy sufficient for the realisation of inelastic collisions in the active medium. In this case, the amplitude of the phantom current can achieve 60 % of the maximum current flowing through the active medium of the laser, which gives no way of determining unambiguously the nature of phantom currents.

N.A. Yudin West-Siberian Branch, Russian State University of Innovation Technologies and Enterprise, prosp. Lenina 36, 634050 Tomsk, Russia; e-mail: yudin@tic.tsu.ru;
V.B. Sukhanov Institute of Atmospheric Optics, Siberian Branch, Russian Academy of Sciences, prosp. Akademicheskii 1, 634055 Tomsk, Russia;
F.A. Gubarev, G.S. Evtushenko Institute of Atmospheric Optics, Siberian Branch, Russian Academy of Sciences, prosp. Akademicheskii 1, 634055 Tomsk, Russia; Tomsk Polytechnic University, prosp. Lenina 30, 634050 Tomsk, Russia

Received 16 April 2007
Kvantovaya Elektronika **38** (1) 23 – 28 (2008)
Translated by M.N. Sapozhnikov

In this paper, we studied the nature of phantom currents by investigating the dependences of the amplitude and duration of currents flowing in the discharge circuit of the laser on the parameters of the active medium and excitation conditions.

2. Simulation of processes in the discharge circuit of a laser

The initial stage of the discharge development and processes proceeding on electrodes and in near-electrode regions of the gas-discharge tube (GDT) in repetitively pulsed self-contained metal atom transition lasers have not been considered in fact, which complicates the simulation of the kinetics of processes proceeding in the active medium of such lasers. The active medium of the laser is usually specified in simulations as a load with lumped parameters. The load is represented by two series-connected elements determining the active and inductive components of the GDT impedance; a peaking capacitance is connected in parallel with them [2, 3]. The laser GDT consists of a discharge channel with electrodes located on its ends in cold buffer regions [2 – 4]. The laser GDT also has its own capacitance with respect to ground, which should be taken into account during simulations of processes in the discharge circuit. Figure 1 presents the electric circuit of the laser in which the equivalent GDT circuit is shown inside the dashed contour. The active, capacitive, and inductive components of the GDT impedance are represented by series-connected $R - L - C$ circuits, where L_1 and L_3 are the inductances of the GRD current leads; and R_2, L_2, and C_2 are the active, inductive, and capacitive components of the impedance of the GDT active medium, respectively; R_1, R_3, C_1, and C_3 are the active and capacitive components of electrode units with respect to

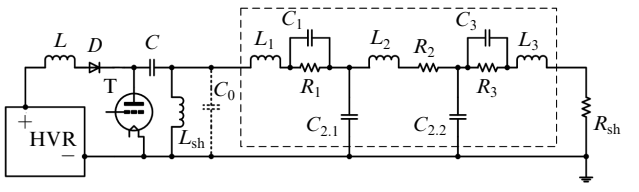

Figure 1. Circuit of the pump oscillator of the laser (the equivalent GDT circuit is shown inside the dashed contour): HVR: high-voltage rectifier; L and D: the charging coke and diode, respectively; C: storage capacitor; C_0: peaking capacitor; T: thyratron; L_{sh}: shunt inductance; R_{sh}: measuring shunt (Rogowski loop).

the active medium, respectively. A storage capacitor C in the laser is charged from a high-voltage rectifier (HVR) through a charging choke L, a diode D and shunt inductance L_{sh}. Then, a trigger pulse is fed to the grid of a thyratron T, and the storage capacitor is connected to the GDT electrodes.

To study processes in the discharge circuit of the laser (Fig. 1), it is necessary to determine the main parameters that should be controlled to provide the unambiguous interpretation of these processes. To do this, it is necessary to envision at least qualitatively the picture of processes proceeding in the discharge circuit of the laser. We used for this purpose computer programs applied for analysis of transient processes in electrotechnical circuits. The initial state of the active components of the GDT impedance was specified in calculations as a prepulse resistance R_0, while the final state of the active components was specified as the mean plasma resistance R_m. The latter is defined as a resistance in which energy equal to that supplied to the active medium during the excitation pulse is released [5, 6]. The plasma resistance was varied in calculations from R_0 to R_m with a certain delay, which was varied during simulations.

Figure 2 presents the results of simulation of the voltage across the GDT and currents flowing through the shunt resistance R_{sh} and thyratron under the following initial conditions: the voltage across the HVR was 6 kV, the excitation pulse rate was $f \sim 17$ kHz, and the capacitance of the storage capacitor was 1300 pF. The dependences presented in Fig. 2 show that processes proceeding in the active medium of repetitively pulsed lasers can be judged by controlling simultaneously the currents flowing through the GDT and thyratron, the voltage across the GDT, and laser radiation parameters. In the given case, the capacitive components of the GDT impedance were charged by discharging the storage capacitor. Because the capacitors C_2 and C_3 are parallel-connected at the initial moment and are connected in series with the capacitor C_1, the latter is charged to a higher voltage. As a result, the breakdown of the cathode–active medium gap occurs earlier. The energy stored in the capacitor C_1 maintains the discharge in this gap, its resistance drastically decreases and shunts the capacitor C_1. Then, a similar process occurs in the active medium–anode gap. Until this moment, the charging current of capacitors C_2 and C_3 flows through the active medium; this current is detected as the phantom current and is in fact the charge displacement current. In this case, all the regions of the active medium should be at the same potential and, therefore, prepulse electrons cannot acquire the energy sufficient for providing inelastic collisions in the active medium. Because the charging current of capacitors C_1 and C_2 does not flow in the given case through the measuring shunt R_{sh}, the currents flowing through the thyratron and active medium are initially considerably different.

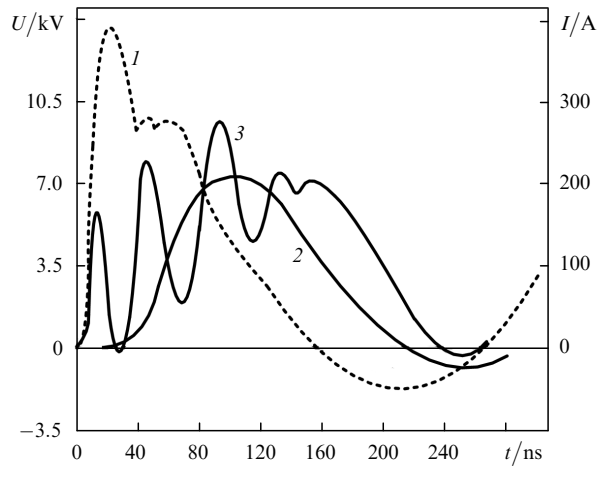

Figure 2. Simulated voltage pulses across the GDT (*1*) and current pulses flowing through the GDT (*2*) and thyratron (3).

The simulated time dependences of currents flowing through the GDT and thyratron showed that the absolute value of the current from the GDT cathode can exceed the current flowing through the active medium. Note that the intrinsic capacitance C_2 of the GDT active medium is a distributed capacitance, which is denoted by $C_{2.1}$ and $C_{2.2}$ in the equivalent circuit. This capacitance can be charged either from the GDT cathode side (the first operation regime considered above) or from the GDT anode side (the second operation regime). In the first case, the capacitor C_2 is charged by the charge displacement current along the active medium from the GDT cathode to its anode, while in the second case – by the charging current of the capacitive component of the GDT impedance from the anode to cathode. In this case, as follows from simulations of this process, currents flowing through the measuring shunt and thyratron should flow simultaneously, but the amplitude of current flowing through the measuring shunt should exceed that of current flowing through the thyratron. At first glance, this looks like nonsense, because in this case the charging current of the capacitive component of the GDT would flow along the way of greatest resistance; however, this is confirmed experimentally and can be explained physically.

3. Experimental results

We studied the dependences of the amplitude and duration of phantom currents on the parameters of the active medium and excitation conditions by using a CuBr–Ne–H_2(HBr) laser with parameters comparable to those of a HyBrID laser [2, 7, 8]. This laser was chosen because HyBrID and CuBr–Ne–H_2(HBr) lasers have the higher prepulse plasma resistance than Cu and CuBr lasers [2, 9]. This allows one to obtain phantom currents of maximum duration, which simplifies somewhat experiments.

We investigated a GDT with a discharge channel diameter of 58 mm and a discharge gap length (interelectrode distance) of 105 cm. The active region was placed into an external heater made in the form of a rectangular metal housing with a thermal insulation layer and a built-in heating element. Such a construction allowed us to maintain the temperature of the working volume at the optimal level (760–800 °C) irrespective of the pump conditions. Approximately 10 cm of the discharge gap on each side of the GDT were outside the heater. The distance between the GDT wall and the metal part of the housing was 60–90 mm. Three containers with the working substance CuBr were uniformly arranged along the active region length; they were placed outside the external heater and were heated independently. The working temperature of containers was selected by the maximum of the output laser power. To introduce HBr into

the active medium, a container with an adsorbent saturated with HBr (HBr generator) was used which was located on the GDT anode side and had an individual heat controller. The container temperature was maintained at the level corresponding to the maximum output laser power, i.e. to the optimal amount of added HBr [8]. Studies were performed at a buffer neon gas pressure of ~ 4 kPa, an excitation pulse repetition rate of 17 kHz, and a storage capacitor of 1300 pF. A TGI1-1000/25 thyratron was used as a switch. The voltage across the GDT was measured with a noninductive ohmic divider, and currents flowing through the active medium and thyratron were measured with Rogowski loops and a Tektronix TDS-3032 oscilloscope. The inverse voltage across the thyratron anode was measured with a static kilovoltmeter.

As the voltage across the HVR was increased from 4.0 to 6 kV, the average output power increased from 5 to 15 W [curve (*4*) in Fig. 3]. In this case, the power supplied from the HVR varied from 0.8 to 2.4 kW. The maximum laser efficiency ~ 0.84 % was achieved in the voltage range across the rectifier from ~ 4.5 to 5.0 kV [curve (*5*)]. A nonlinear variation in the maximum voltage amplitude across the GDT was observed [curve (*1*) in Fig. 4], while the inverse voltage across the thyratron anode increased almost linearly [cure (*2*)]. The rise time of voltage across the GDT to its maximum changed from 24 to 80 ns [curve (*1*) in Fig. 3], and the time delay of the lasing onset was observed [curve (*2*)].

Oscillograms of voltage pulses across the GDT and laser pulses and current pulses flowing through the measuring GDT shunt and thyratron are presented in Figs 5 and 6. The first operation regime (Fig. 5) was observed at voltages across the HVR up to 5 kV. At the voltage 5.5 kV, the first operation regime gradually passed to the second one, and beginning from 6 kV, the second operation regime was observed (Fig. 6). An increase in the voltage across the HVR above 6 kV resulted in the unstable operation of the thyratron in the discharge circuit of the laser. As the voltage across the HVR was increased from 4.0 to 6.0 kV, the FWHM of laser pulses slightly decreased [curve (*3*) in Fig. 3]. The laser pulse amplitude and pulse base duration changed more noticeably (Fig. 7).

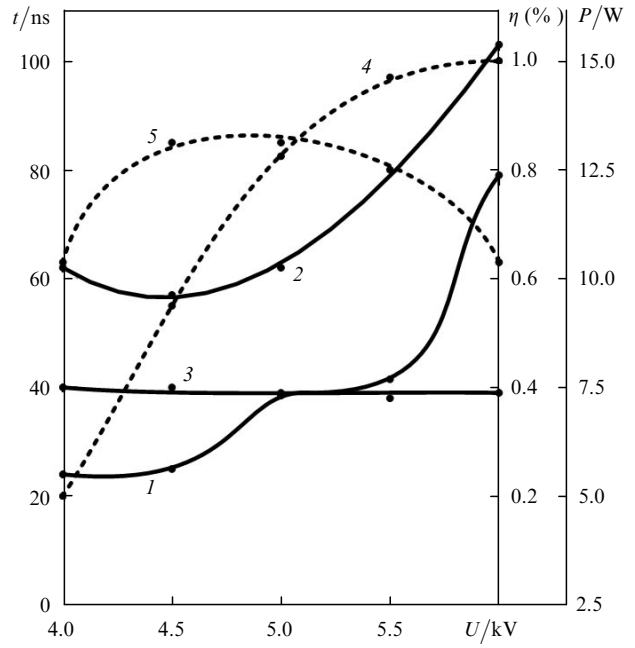

Figure 3. Dependences of the rise time of voltage across the GDT (*1*), the lasing onset time (*2*), the laser pulse FWHM (*3*), the average laser power (*4*), and the laser efficiency η (*5*) on the voltage across the HVR.

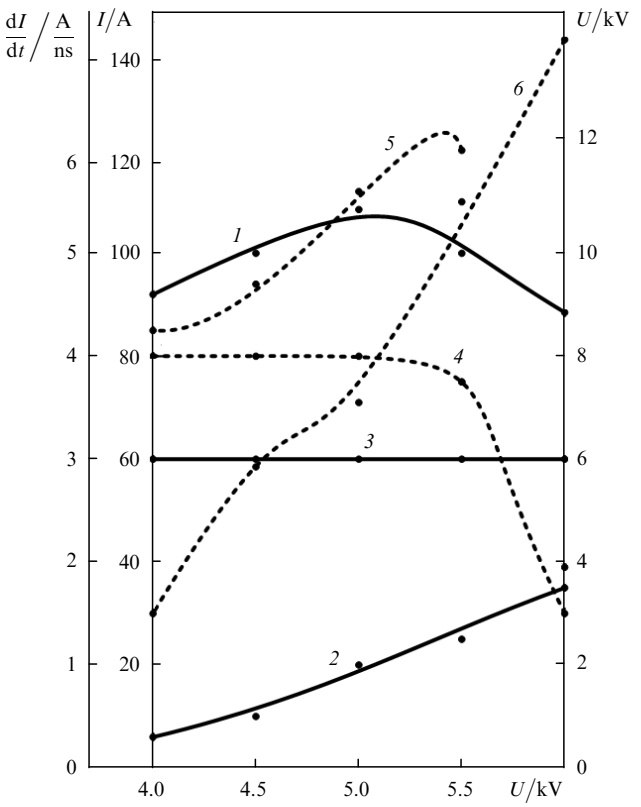

Figure 4. Dependences of the maximum amplitude of voltage across the GDT (*1*), the inverse voltage across the thyratron anode (*2*), the voltage across the GDT at which lasing begins (*3*), the current rise rate in the thyratron (*4*), the charging current amplitude of the capacitive components of the discharge circuit impedance (*5*), and the current amplitude flowing through the GDT by the lasing onset (*6*) on the voltage across the HVR.

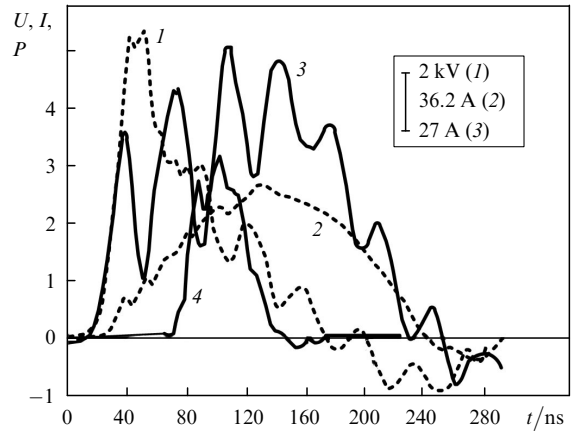

Figure 5. Oscillograms of the voltage pulse across the GDT (*1*), current pulses flowing through the GDT (*2*) and thyratron (*3*), and the laser pulse (*4*), corresponding to the first operation regime (voltage across the rectifier is 4.5 kV).

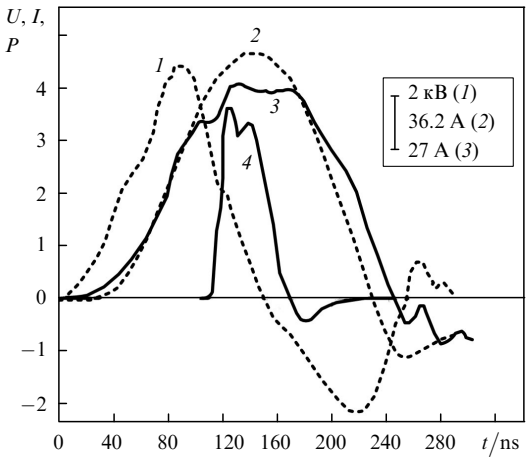

Figure 6. Oscillograms of the voltage pulse across the GDT (*1*), current pulses flowing through the GDT (*2*) and thyratron (*3*), and the laser pulse (*4*), corresponding to the second operation regime (voltage across the rectifier is 6.0 kV).

4. Discussion of results

Our study has shown that the current flowing through the thyratron in the first operation regime is caused by the charging of the capacitive component C_i of the GDT impedance, which is determined from the equivalent GDT circuit (Fig. 1):

$$\frac{1}{C_i} = \frac{1}{C_1} + \frac{1}{C_2 + C_3}. \qquad (1)$$

As the voltage across the HVR was increased from 4.0 to 6.0 kV, the charging time of C_i increased [curve (*1*) in Fig. 3]. The current rise rate remains constant ~ 4 A ns^{-1} [curve (*4*) in Fig. 4] until the change in the operation regime. Because the admissible current rise rate for the TGI1-1000/25 is ~ 4 A ns^{-1} [10], we can conclude that the charging rate and time of the capacitor C_i are virtually determined by the thyratron rather than by the parameters of the discharge circuit of the laser, which is confirmed by the observed dependence [curve (*1*) in Fig. 4]. It is known that the voltage across the storage capacitor in the laser under study exceeds the double voltage across the HVR by the inverse voltage across the thyratron anode [5, 6]. Curve (*1*) in Fig. 4 shows that the voltage across the capacitor C_i exceeds the voltage across the storage capacitor only when the voltage across the rectifier is ~ 4.0 kV, i.e. upon charging the capacitor C_i, there exits an insignificant contribution of the inductive component of the impedance of the laser discharge circuit. Knowing the voltage U to which the capacitor C_i is charged, the storage time t, the current amplitude I, and taking into account a linear increase of current in the charging circuit, we can determine the value of C_i:

$$C_i = \frac{q}{U} = \frac{It}{2U}. \qquad (2)$$

By substituting into (2) the parameters $U = 10$ kV, $t = 24$ ns, and $I = 97$ A obtained from oscillograms in Fig. 5, we obtain $C_i = 116.4$ pF. The phantom current in the active medium of the laser is observed until the 'active

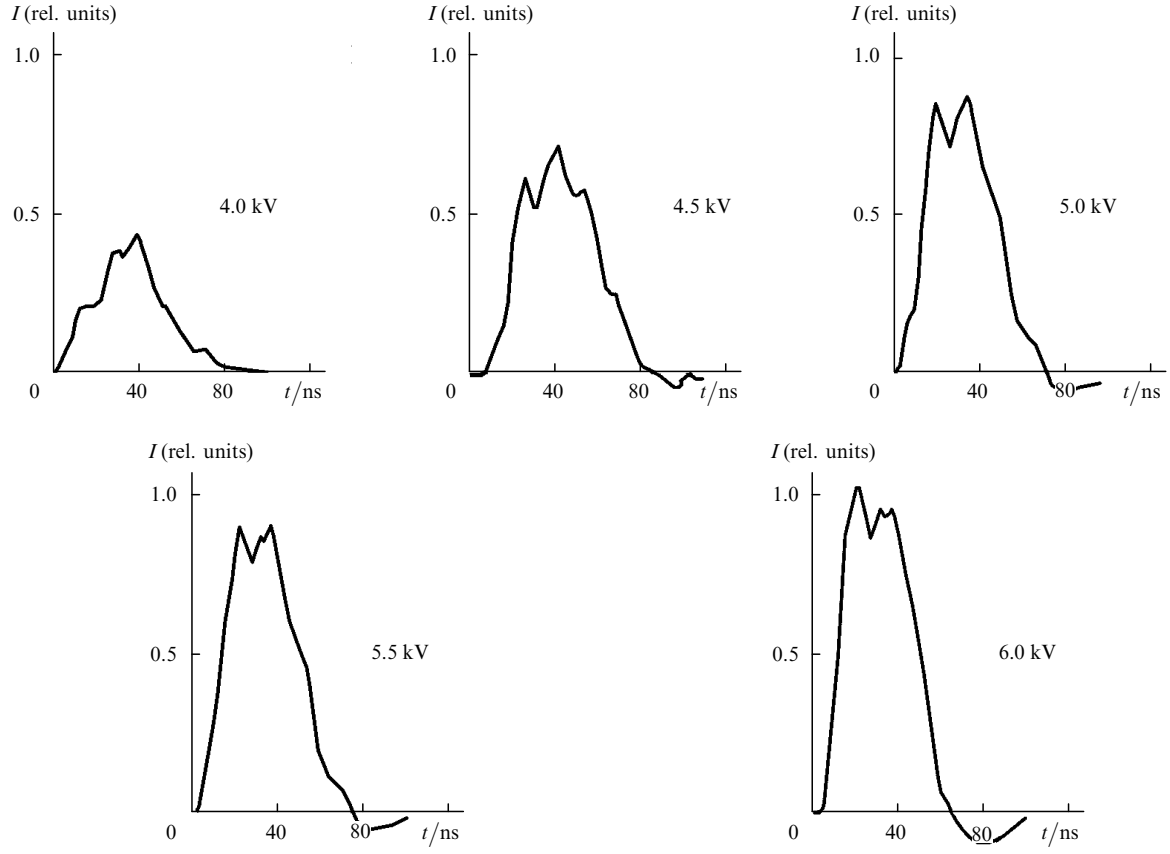

Figure 7. Laser pulses for different voltages across the HVR.

medium breakdown' [1], which is in fact the breakdown of the anode–active medium gap. If it is the case, the breakdown of this gap should occur after a certain voltage across the GDT is achieved irrespective of the voltage across the HVR. It was shown in [1, 11] that lasing appears after the 'active medium breakdown'. Measurements showed that lasing always began in our case when the voltage across the GDT achieved ~ 6 kV [curve (*3*) in Fig. 4]. Because the GDT electrode units are identical, we can confidently assume that the breakdown of the cathode–active medium gap also occurs at the voltage ~ 6 kV. This allows us to estimate the GRD capacitances C_1, C_2, and C_3. By the instant of the cathode–active medium gap breakdown (Fig. 5), we have $U_{C_i} = 10$ kV, $U_{C_1} = 6$ kV, $U_{C_2} = 4$ kV, $U_{C_3} = 4$ kV. By assuming that $C_1 = C_3$, we find $C_1 = C_3 \sim 190$ pF and $C_2 \sim 100$ pF. Because the charge of the capacitor C_i is determined by the thyratron, while the current rise rate is independent of the voltage across the GDT and is 4 A ns^{-1}, this is equivalent to the charging of the capacitor C_i through a resistance, which can be estimated as $R = t/C_i \sim 200$ Ω.

Our study and estimates made in the paper suggest that the phantom current is caused by the specificity of charging capacitive components of the discharge circuit impedance of the laser. However, for the above interpretation of physical processes to be reliable, it is necessary to know that all the capacitive components of the discharge circuit impedance have been taken into account in model calculations. Based on the estimates presented above, the capacitances of the electrode units are $C_1 = C_3 \sim 190$ pF, which is an order of magnitude higher than the value calculated assuming that the capacitance of the electrode unit represents a flat capacitor. In this case, the equivalent GDT capacitance C_i should be ~ 10 pF. A considerable discrepancy in the estimates of electrode unit capacitances suggests that processes can exist in the GDT and discharge circuit of the laser that enlarge the volume discharge of electrode units, which is, however, unlikely, or not all the capacitive components are taken into account. In particular, the capacitance of buses supplying current to the GDT may be neglected. Indeed, the capacitance of current buses with the connected GDT during direct measurements was ~ 120 pF, whereas this capacitance with the disconnected GDT was ~ 110 pF (denoted by C_0 in Fig. 1). Therefore, the equivalent capacitance $C_i \sim 116.4$ pF obtained from volt–ampere characteristics of the discharge determines actually the capacitance C_g of the discharge circuit, which is the sum of $C_0 \sim 100 - 110$ pF and $C_i \sim 5 - 10$ pF. The simulation of processes in the discharge circuit (Fig. 1) taking these values into account gave the result similar to that presented in Fig. 2. However, the interpretation of physical processes proceeding in the laser discharge circuit differs somewhat from that presented above.

Immediately after the thyratron triggering, the accumulation of energy begins in the capacitive components C_0 and C_i of the discharge circuit impedance. In this case, the current flowing through the GDT is the charging current of the capacitive component C_i of the GDT impedance, while the current flowing through the thyratron at this time is the charging current of the capacitive component $C_g = C_0 + C_i$ of the discharge circuit impedance of the laser, which results in a considerable difference between currents flowing through the thyratron and GDT. Because the capacitance C_1 is connected in series with capacitances C_2 and C_3, it is charged to a higher voltage. When the voltage across the capacitor C_1 achieves ~ 6 kV, the breakdown of the active medium-cathode discharge gap occurs. In this case, the voltage across the capacitance C_0 is ~ 10 kV and capacitances C_2 and C_3 are charged to the voltage ~ 4 kV and are connected in parallel with the capacitance C_0. Because the capacitive components of the discharge circuit impedance are charged through the thyratron with the admissible current rise rate ~ 4 A ns^{-1}, which is equivalent to the charging via a resistance of ~ 200 Ω, and this rate cannot increase, the charge is redistributed between capacitances C_0, C_2, and C_3. In this case, the decrease in the voltage across the GDT and current flowing through the thyratron is observed (Fig. 5). According to the law of conservation of charge, we find that $C_2 + C_3 \sim 110$ pF, or $C_2 \sim 90 - 100$ pF and $C_3 = C_1 \sim 10 - 20$ pF. Then, the capacitive components C_0, C_2, and C_3 are charged up to the breakdown voltage of the active medium–anode gap.

Because the charging of the capacitor C_g is determined by the thyratron, while the current rise rate is independent of the voltage across the HVR, being equal to ~ 4 A ns^{-1}, this is equivalent to the charging of the capacitor C_g through a resistance increasing with voltage across the rectifier. When the equivalent resistance of the thyratron becomes comparable with the prepulse plasma resistance, the first operation regime passes to the second one (Fig. 6). In our case, this transition occurs when the voltage across the rectifier achieves $\sim 5.5 - 6.0$ kV. Oscillograms in Figs 5 and 6 show that the voltage rise rate across the GDT in the second regime decreases and no charge redistribution between capacitances C_0 and C_2 is observed, which is equivalent to their charging through the resistance R_1. Knowing the charging time of capacitors C_0 and C_2 and taking into account that $t = R(C_0 + C_2)$, we can estimate the prepulse plasma resistance in the active medium–cathode gap as ~ 500 Ω. In this case, the prepulse electron concentration n_e determined from the plasma conductivity is $\sim 2 \times 10^{11}$ cm^{-3}, which is an order of magnitude lower than its typical value in the active medium of the laser. Taking into account that C_2 is a distributed capacitance, this determines the equality of potentials in the active medium during the charging of the capacitive components of the discharge circuit impedance of the laser in the first and second operation regimes.

5. Conclusions

Our study and estimates have shown that:

(i) The phantom current is caused by the specific nature of charging the capacitive component of the GDT impedance of the laser. During the phantom current existence, the active medium is at the equal potential, which prevents prepulse electrons from accumulating the energy required to realise inelastic collisions in the active medium.

(ii) Because of a low admissible current rise rate in the thyratron, the operation regime is realised in which the capacitive component of the discharge circuit impedance of the laser is charged through the active medium. Because the first and second laser operation regimes are equivalent with respect to the charging of the capacitive component of the discharge circuit impedance, the active medium should be at the equal potential in the second regime as well during the existence of the phantom current.

(iii) The capacitive components of the discharge circuit

of the laser and GDT can considerably affect the energy characteristics of the laser and kinetics of processes proceeding in the active medium, which requires further, more detailed studies.

Acknowledgements. This work was supported by the Ministry of Defence of the Russian Federation (Project No. RNP2.1.1.5450).

References

1. Hogan G.P., Webb C.E. *Opt. Commun.*, **117**, 570 (1995).
2. Little C.E. *Metal Vapour Lasers. Physics, Engineering and Applications* (New York: John Wiley & Sons, 1999) p. 620.
3. Batenin V.M., Buchanov V.V., Kazaryan M.A., Klimovskii I.I., Molodykh E.I. *Lazery na samoogranichennykh perekhodakh atomov metallov* (Self-Contained Metal Atom Transition Lasers) (Moscow: Nauchnaya kniga, 1998).
4. Grigor'yants A.G., Kazaryan M.A., Lyabin N.A. *Lazery na parakh medi. Konstruktsiya, kharakteristiki i primeneninya* (Copper Vapour Lasers: Design, Parameters, and Applications) (Moscow: Fizmatlit, 2005).
5. Kel'man V.A., Klimovskii I.I., Fuchko V.Yu., Zapesochnyi I.P. Preprint KIYaI No. 85 (Kiev, 1985).
6. Yudin N.A. *Kvantovaya Elektron.*, **25**, 795 (1998) [*Quantum Electron.,* **28**, 774 (1998)].
7. Zemskov K.I., Isaev A.A., Petrash G.G. *Kvantovaya Elektron.*, **24**, 596 (1997) [*Quantum Electron.,* **27**, 579 (1997)].
8. Shiyanov D.V., Evtushenko G.S., Sukhanov V.B., Fedorov V.F. *Kvantovaya Elektron.*, **37**, 49 (2007) [*Quantum Electron.*, **37**, 49 (2007)].
9. Hogan G.P., Webb C.E., Whyte C.G., Little C.E., in *Pulsed Metal Vapour Lasers*. Ed. by C.E. Little and N.V. Sabotinov (New York: Kluwer Acad. Publ., 1995) Vol. 5, p. 67.
10. Kantsel'son B.V., Kalugin A.M., Larionov A.S. *Elektrovakuumnye elektronnye i gazorazryadnye pribory* (Vacuum Electronic and Gas-Discharge Instruments) (Moscow: Radio i Svyaz', 1985).
11. Evtushenko G.S., Kostyrya I.D., Sukhanov V.B., Tarasenko V.F., Shiyanov D.V. *Kvantovaya Elektron.*, **31**, 704 (2001) [*Quantum Electron.*, **31**, 704 (2001).